8.8 Miniaturization of Magnetic Resonance Microsystem Components for 3D Cell Imaging

Long-Sheng Fan, Shawn S. H. Hsu, Jun-De Jin, Cheng-Yu Hsieh, Wei-Chen Lin, H. C. Hao, Hsin-Li Cheng, Kuo-Chin Hsueh, Chen-Zong Lee

National Tsing Hua University, Hsinchu, Taiwan.

Nuclear magnetic resonance imaging (MRI) is a powerful tool for non-invasive 3D imaging. Since the precession frequency of a nucleus is linearly proportional to the local magnetic field, a constant spatial gradient field generated by a gradient coil encodes the location of a signal. The imaging is achieved by spatially coding the precession frequencies/phases of nuclear magnetic moments of the sample with a set of gradient coils under a bias magnetic field and using RF coils to excite in a certain specified sequence and then detect signals from these magnetic moments. The 3D images are reconstructed after localization of the RF signal in a signal processor. In medical diagnosis, an MRI resolution of a few millimeters is typically adequate; however, if the subject under study is a cluster of cells such as a live embryo, then the availability of high resolution 3D live-cell imaging at low cost is desirable.

Through the reciprocal theorem in electromagnetic theory, the voltage induced in the RF receiver coil is:

$$V(t) = -\frac{\partial}{\partial t} \int_{sample} B_1(\vec{r}) \cdot M_0(\vec{r},t) dV_S$$

where $B_1(\vec{r})$ is the magnetic field at point $\vec{r}$ generated by the receiver coil with a unit current, $M_0(\vec{r},t)$ is the magnetic moment density at point $\vec{r}$ and dV is the associated differential volume. $B_1(\vec{r})$ generated by a unit current is inversely proportional to the size scaling factor according to Ampere's Law. Thus, the mass sensitivity of an RF coil also scales inversely with the size scaling factor, and the miniaturization of the RF receiver coils has been utilized to achieve high mass sensitivity in magnetic resonance spectroscopy [1]. Manually wound individual RF coils with a precision jig under microscopes has also been used in imaging and achieved impressive laboratory results [2]; however, manufacturing thousands to millions of complete devices with the required precision and reproducibility with low cost for high throughput applications requires new manufacturing approaches. There were several microfabrication efforts mostly with planar coils for spectroscopy applications such as in [3]. Also, a much less utilized fact is that the magnetic field gradients scale with the inverse square law and the resultant high magnetic field gradient is essential in achieving high imaging resolution.

To implement compact imaging systems, magnetic resonance components are presented that are miniaturized and integrated, including gradient coils and RF coils, using a lithography-based batch fabrication process [4,5]. Scaling laws are exploited in the MRI imaging components to produce initial imaging results using this approach. Also integrated is the associated RF transceiver front-end components to achieve better signal-to-noise performance. While the signal sensitivity is increased due to the scaling law, the noise for the MRI system at such dimensions is dominated by electronic noise of the receiver and the thermal noise of the RF coil, which essentially remains constant with the coil resistance as determined by the skin depth. Figure 8.8.1 shows the schematics of the gradient coils to produce uniform magnetic field gradients. The gradient coils, consisting of two sets of four 120-degree saddle coils, are arranged in a way such that they produce uniform gradients in two orthogonal directions and a set of Maxwell coils that produces the uniform field gradients in the third orthogonal direction. In the center of the gradient coils is a cylindrical sample chamber with access from the top surface.

Figure 8.8.2 shows microfabricated saddle coils in two orthogonal directions currently under characterization and the 3D finite element analysis of the magnetic fields using HFSS analysis. An 800μm diameter micro RF coil using a commercial 0.9T/m gradient coils and a gradient echo sequence is used for preliminary imaging study and a resolution of 6×6μm^2 in a 120μm slice is achieved and images of live onion cell walls are obtained as shown in Fig. 8.8.3.

Figure 8.8.4 shows the simplified MRI system diagram, where one of the dotted boxes indicates the RF transceiver front end and the other is the MEMS chip including the RF and gradient coils. The custom-made digital console consists of the transmitter, the receiver, the signal averager, the pulse programmer, the gradient controller and the digital signal processor. The gradient coil driver converts the voltage output of gradient controller to driving currents used in the gradient coils. The external magnet with an 8 inch diameter for the MRI system is also shown.

Figure 8.8.5 shows the circuit schematic of the integrated RF transceiver chip including the LNA, the switches, and the power amplifier. Figure 8.8.6 is a micrograph of the chip that has been fabricated in a 0.18μm CMOS process. The LNA is designed with a cascaded common-source configuration to meet the design specifications of 20dB gain and 2dB noise figure at the operation frequencies with both input/output reflection coefficients (S_{11} and S_{22}) below -20dB. The PA and LNA are designed with shunt-shunt feedback for a wideband characteristic to cover the frequencies of 77MHz, 125MHz, and 500MHz. The measured result of the PA shows a maximum power of 20dBm with a gain of 17dB at 500MHz, which is adequate to drive the MRI microcoil. The switch is designed with both shunt- and series-connected transistors for better Tx/Rx isolation, and the measured insertion loss and isolation are below 2.0dB and above 30dB at the frequencies of interest. Using the CMOS chip and the microcoil, the measured magnetic-resonance spectrum of glucose deuterium water solution shows the characteristic peaks as evidenced in Fig. 8.8.7. The batch fabricated MEMS miniaturized MRI chip and the transceiver front end chip implemented using a 0.18μm CMOS technology can replace high-cost MRI counterparts for micron-resolution 3D images of clusters of live cells (which can be optically opaque) and enables a desk-top cellular MRI system with micron resolution. Since the MEMS portion is made in a low temperature process, the MEMS coils can be co-integrated with the CMOS circuits, if desired.

Acknowledgments:
The authors would like to thank National Chip Implementation Center (CIC), Hsinchu, Taiwan, for chip implementation and measurement.

References:
[1] D. L. Olson et al., "High-Resolution Microcoil ^{1}H-NMR for Mass-Limited, Nanoliter-Volume Samples," *Science,* vol. 270, pp. 1967-1970, Dec., 1995.
[2] L. Ciobanu et al, "3D Micron-Scale MRI of Biological Cells," *Solid State Nucl. Magn. Reson.,* vol. 25, pp. 138-141, Jan., 2004.
[3] C. Massin et al, "High-Q factor RF Planar Microcoils for Micro-Scale NMR Spectroscopy," *Sensors & Actuators A: Physical,* vol. 97, pp. 280-288, Apr., 2002.
[4] Long-Sheng Fan, "NanoMR (Magnetic Resonance) for Molecular and Cellular Studies," *Abstracts of the Fourth International Symposium on Microchemistry and Microsystems,* pp. 18-19, Nov., 24-26, 2004.
[5] Long-Sheng Fan et al., "Magnetic Resonance Microsystems for Life Science Applications," *Proc. of Transducers 2005,* pp. 1998-2001, June, 2005.

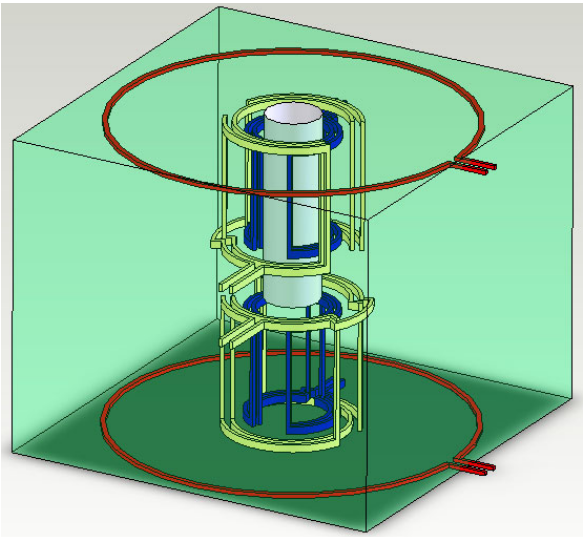

Figure 8.8.1: A multi-layer metal gradient coil design that produces uniform magnetic field gradients in three orthogonal directions.

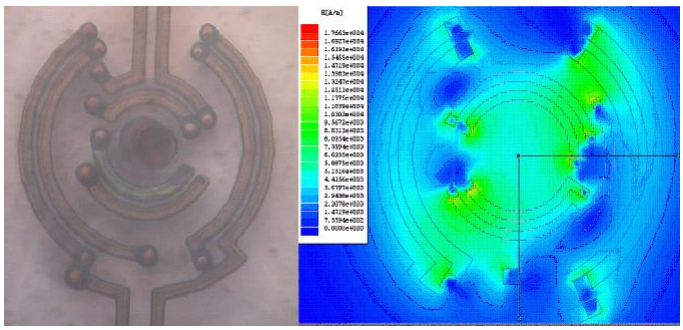

Figure 8.8.2: The top view of the microfabricated saddle coils for two orthogonal directions currently under characterization and the 3D HFSS analysis of the magnetic field distribution. The outer diameter of the outside coil is 600μm.

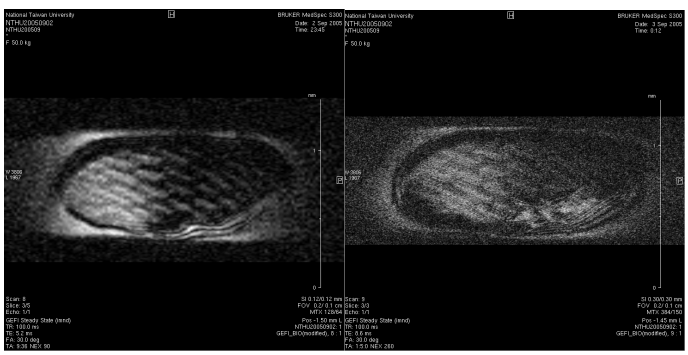

Figure 8.8.3: MRI images show slices of live onion cells with a 6μm×6μm resolution using an 800μm microcoil with a gradient echo sequence. A single cell is around 100μm in width. The cell walls are clearly visible.

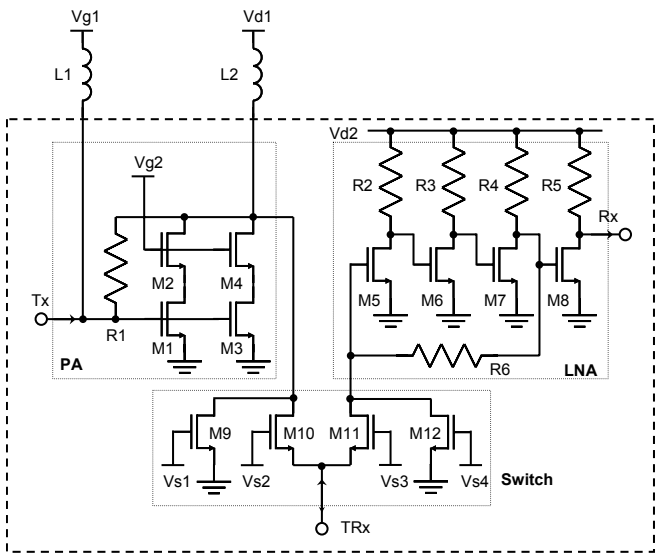

Figure 8.8.5: Circuit architecture of the integrated RF front end for the MRI system.

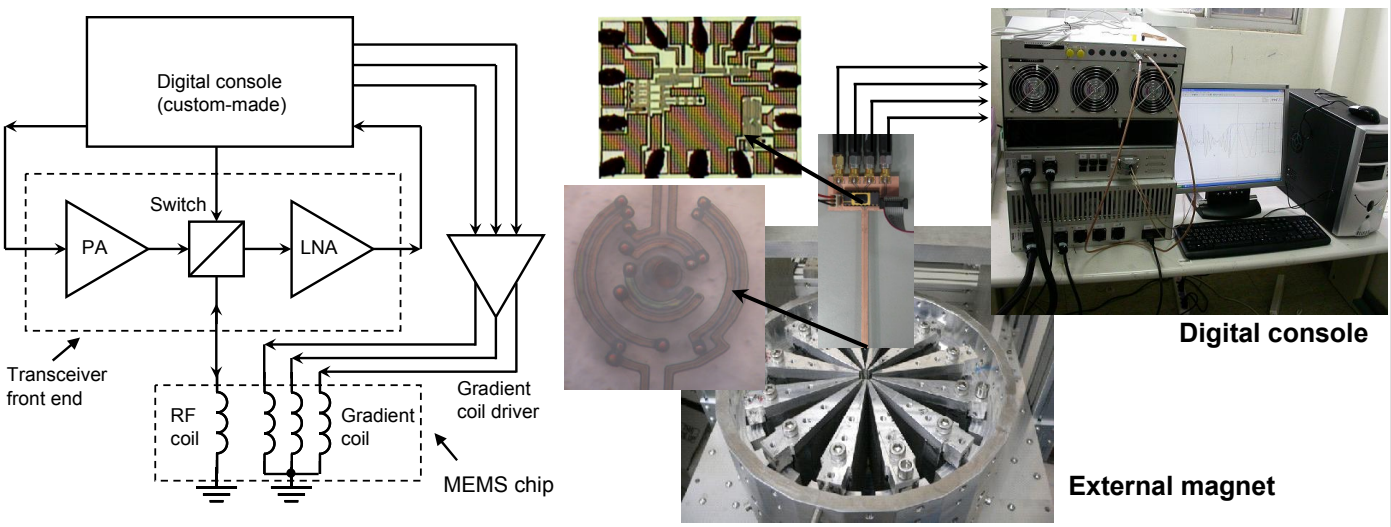

Figure 8.8.4: A desk-top MRI system for cell cluster observation.

Continued on Page 594

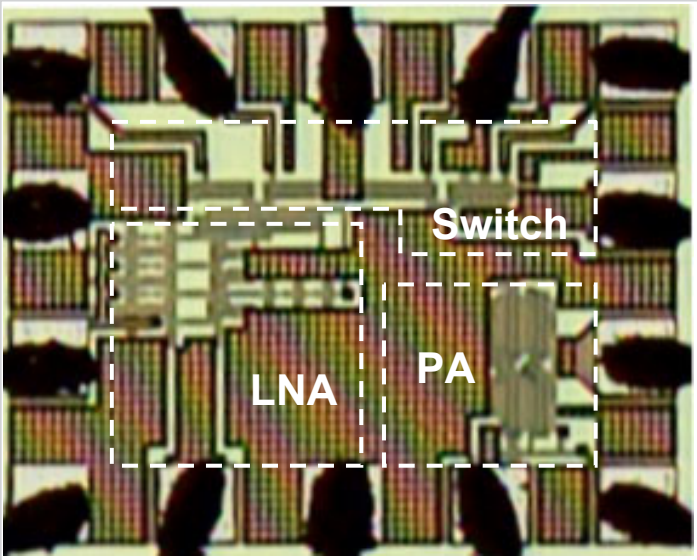

Figure 8.8.6: Chip micrograph.

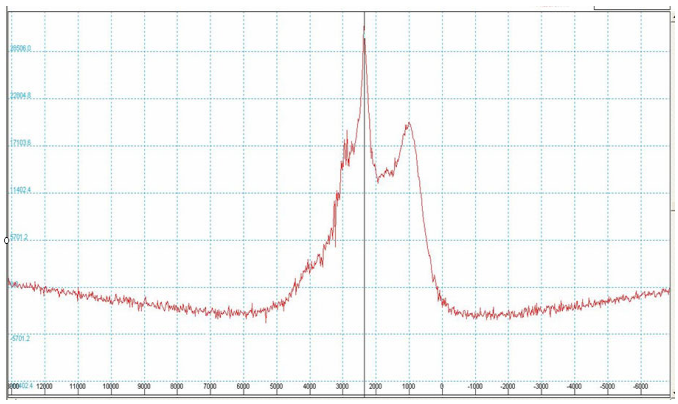

Figure 8.8.7: The measured magnetic-resonance spectrum of glucose deuterium water solution which shows the characteristic peaks from water and glucose.

